Pattern formation in quantum Turing machines

Ilki Kim* and Günter Mahler
Institut für Theoretische Physik, Universität Stuttgart, Pfaffenwaldring 57, 70550 Stuttgart, Germany
(Received 10 December 1998)

We investigate the iteration of a sequence of local and pair unitary transformations, which can be interpreted to result from a Turing-head (pseudospin S) rotating along a closed Turing tape (M additional pseudospins). The dynamical evolution of the Bloch vector of S, which can be decomposed into 2^M primitive pure state Turing-head trajectories, gives rise to fascinating geometrical patterns reflecting the entanglement between head and tape. These machines thus provide intuitive examples for quantum parallelism and, at the same time, means for local testing of quantum network dynamics. [S1050-2947(99)07905-6]

PACS number(s): 03.67.Lx, 03.65.Bz, 05.45.−a, 89.70.+c

Despite the lack of a clear-cut definition, the physics of *complexity* [1] has intrigued physicists for many years. For continuous classical systems with few degrees of freedom, the notion of chaos has attracted much interest as a sign of uncontrollability [2]. For discrete classical systems in the form of cellular automata, the notion of computational irreducibility has been introduced to account for the lack of ''short cuts,'' i.e., our inability to predict the respective state evolution without following the detailed dynamics step by step [3]. The linearity of quantum dynamics appears to make the respective evolution ''well behaved'' from the start. The limit of control, nevertheless, abounds even for modestly large quantum networks [4] due to the, typically, exponentially large Hilbert space, in which the state evolves [5]. It has been shown that if this kind of ''quantum complexity'' could be harnessed, new efficient modes of computation should become available [6,7]. However, one will first have to find ways to circumvent that disastrous exponential blowup.

A quantum network (composed of N subsystems) is defined by its Hamiltonian operator $\hat{H}$. This $\hat{H}$ is also the generator of the respective unitary (system) dynamics, $\hat{U}(t) = \exp(-i\hat{H}t/\hbar)$, which transforms a given initial state $|\psi_0\rangle$ into a final state $|\psi'\rangle$ after some given time Δt: We thus have a one-parameter transformation $\hat{U}(\Delta t)$ operating on arbitrary initial states (requiring a number of state parameters which grows exponentially with N). To improve control it is therefore tempting to consider, instead, arbitrary unitary transformations acting on one given initial state: In fact, this type of scenario underlies most current quantum-computational schemes [7].

Any system dynamics can be approximated as an iterative sequence of unitary basis operators (so-called ''gates'' [8]). In this Brief Report we address a quantum Turing machine (QTM) architecture [9–13] which can be understood as a specific and formalized version of such an iterative map. Typically, one will be unable to ''observe'' the network in full detail; one then usually resorts to ''macro-observables.'' Here we focus, instead, on a single microscopic subsystem, the ''Turing head'' S. To predict its state exactly, the full network state is required. However, while the evolution of arbitrary initial states by a given map seems exponentially ''hard,'' the evolution of some specific initial state by a whole class of maps turns out to be ''easy,'' and is not at all limited to small-N networks. Furthermore we will show that the evolution of the Turing head in its reduced space gives rise to geometrical patterns reflecting the entanglement between Turing head and Turing tape. These patterns can be thought to result from the superposition of exponentially many ''basic'' Turing machines, an intuitive example of ''quantum parallelism.''

The quantum network to be considered here is composed of N $(=M+1)$ pseudospins $|j(\mu)\rangle$, $j=0,1$; $\mu = S,1,2,\ldots,M$ (Turing head S, Turing tape spins $1,2,\ldots,M$) so that its network state $|\psi\rangle$ lives in the 2^{M+1}-dimensional Hilbert space spanned by the product wave functions $|j(S)k(1)\cdots l(M)\rangle = |jk\cdots l\rangle$. Correspondingly, any (unitary) network-operator can be expanded as a sum of product operators. The latter may be based on the traceless SU(2) generators

$$\hat{\lambda}_x(\mu) = \hat{P}_{01}(\mu) + \hat{P}_{10}(\mu),$$

$$\hat{\lambda}_y(\mu) = i\hat{P}_{01}(\mu) - i\hat{P}_{10}(\mu),$$

$$\hat{\lambda}_z(\mu) = \hat{P}_{11}(\mu) - \hat{P}_{00}(\mu), \tag{1}$$

where $\hat{P}_{ij}(\mu) = |i(\mu)\rangle\langle j(\mu)|$ is a (local) transition operator.

We now consider the iterative map for which each full cycle $p=1,2,\ldots$ consists of a sequence of $2M$ unitary transformations $\hat{U}_n$, $n=1,2,\ldots,2M$. At step m, $m=n+2M(p-1)$, we thus have

$$|\psi_m\rangle = \hat{U}_n\cdots\hat{U}_2\hat{U}_1(\hat{U}_{2M}\cdots\hat{U}_2\hat{U}_1)^{p-1}|\psi_0\rangle. \tag{2}$$

Presently we identify the $\hat{U}_n$ with the local unitary transformation on the Turing head S, $\hat{U}_\alpha(S)$, and the quantum-controlled-NOT (QCNOT) on (S,μ), $\hat{U}(S,\mu)$, respectively:

$$\hat{U}_{2\mu-1} = \hat{U}_{\alpha_\mu}(S) = \hat{1}(S)\cos(\alpha_\mu/2) - \hat{\lambda}_x(S)\,i\sin(\alpha_\mu/2), \tag{3}$$

*Electronic address: ikim@theo.physik.uni-stuttgart.de

$$\hat{U}_{2\mu}=\hat{U}(S,\mu)=\hat{P}_{00}(S)\hat{\lambda}_x(\mu)+\hat{P}_{11}(S)\hat{1}(\mu)=\hat{U}^{+}(S,\mu). \tag{4}$$

However, the basic results of this paper apply also to different transformations $\hat{U}(S,\mu)$, e.g., with $\hat{\lambda}_x(\mu)$ replaced by $i\hat{\lambda}_y(\mu)$. In any case, the sequence of Eq. (2) may be interpreted to emerge from a Turing-head rotation along the closed Turing tape, thus iterating between local and QCNOT operations. Any such QTM is specified by its tape size M, the external control parameters α_μ, $\mu=1,2,\ldots,M$, and the initial state $|\psi_0\rangle$. Without loss of generality we will restrict ourselves to $\alpha_1=\alpha_2=\cdots\alpha_M=\alpha$. The state $|\psi_0\rangle$ will be taken to be a product of Turing-head and -tape wave functions. This initial ''no-correlation'' assumption is typical also for system-bath models [4]. In fact, the Turing tape may be considered as a special (finite) bath model for system S.

We restrict ourselves to the Bloch vector $\vec{\lambda}$ of the Turing head S (our ''system of interest'')

$$\lambda_i^m=\langle\psi_m|\hat{\lambda}_i(S)\otimes\hat{1}(1)\otimes\cdots\otimes\hat{1}(M)|\psi_m\rangle. \tag{5}$$

The Bloch vectors of the Turing tape could be calculated along the same lines, but the Turing head plays a specific role by construction. Due to the entanglement with the Turing tape, the Turing head will, in general, appear to be in a ''mixed state'' $|\vec{\lambda}^m|^2<1$.

The tape spin states

$$|\pm(\mu)\rangle=\frac{1}{\sqrt{2}}(|0(\mu)\rangle\pm|1(\mu)\rangle),\quad \mu=1,2,\ldots,M \tag{6}$$

are eigenstates of $\hat{\lambda}_x(\mu)$ with eigenvalues ±1, respectively. If spin μ is in one of these states, the QCNOT operation

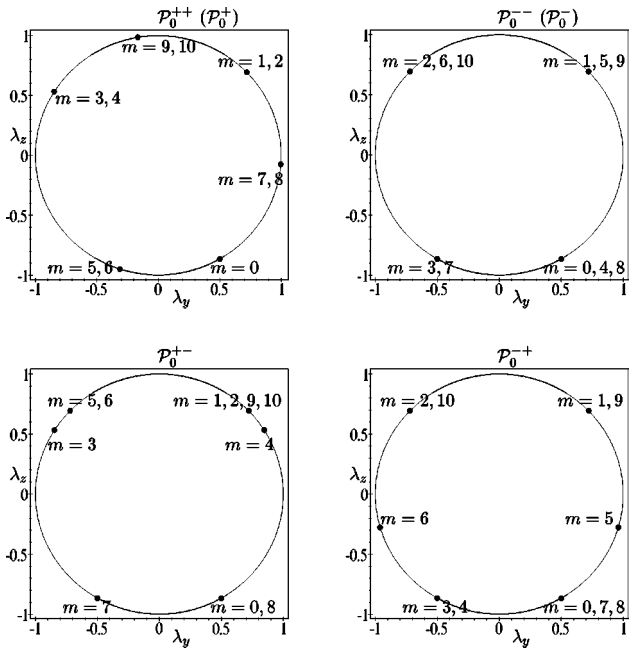

FIG. 1. The primitives $\mathcal{P}_0^{+}$ (aperiodic) and $\mathcal{P}_0^{-}$ (periodic) for $M=1$, and $\mathcal{P}_0^{2+}$ (aperiodic), $\mathcal{P}_0^{2-}$, $\mathcal{P}_0^{+-}$, and $\mathcal{P}_0^{-+}$ (periodic) for $M=2$; $\alpha=\pi/\sqrt{3}$ and $\varphi_0=\pi/6$.

$\hat{U}(S,\mu)$ cannot create any entanglement, irrespective of the head state $|\varphi(S)\rangle$:

$$\hat{U}(S,\mu)|\varphi(S)\rangle\otimes|+(\mu)\rangle=|\varphi(S)\rangle\otimes|+(\mu)\rangle \tag{7}$$

$$\hat{U}(S,\mu)|\varphi(S)\rangle\otimes|-(\mu)\rangle=\hat{\lambda}_z(S)|\varphi(S)\rangle\otimes|-(\mu)\rangle. \tag{8}$$

For the 2^M orthonormalized initial tape states,

$$|\mathcal{P}_0^j\rangle\in\{|\mathcal{P}_0^{\pm\pm\cdots\pm}\rangle=|\pm(1)\rangle\otimes|\pm(2)\rangle\otimes\cdots\otimes|\pm(M)\rangle\} \tag{9}$$

and with $|\varphi_0(S)\rangle=\cos(\varphi_0/2)|0(S)\rangle-i\sin(\varphi_0/2)|1(S)\rangle$, the network state $|\psi_m\rangle$ remains a product state,

$$|\psi_m\rangle=|\varphi_m(S)\rangle\otimes|\mathcal{P}_0^j\rangle, \tag{10}$$

and the Turing head described by

$$\lambda_i^m(\mathcal{P}_0^j)=\langle\mathcal{P}_0^j|\langle\varphi_m(S)|\hat{\lambda}_i(S)\otimes\hat{1}(1)\otimes\cdots\otimes\hat{1}(M)|\varphi_m(S)\rangle|\mathcal{P}_0^j\rangle \tag{11}$$

performs a pure state trajectory on the Bloch circle,

$$(\lambda_y^m(\mathcal{P}_0^j))^2+(\lambda_z^m(\mathcal{P}_0^j))^2=1. \tag{12}$$

We show examples for $\varphi_0=\pi/6$ and $M=1$ and 2 (Fig. 1). The step number m is marked to specify the apparent ''jumping.'' The explicit machine rules for the Turing head are given in Table I ($M=1$). The orbits for tape M are contained in those for $kM(k=2,3,\ldots)$.

For given Turing-tape size M the initial state $|\mathcal{P}_0^j\rangle$ gives rise to a periodic orbit whose period does not depend on α, if

$$|\mathcal{P}_0^j\rangle=|+\rangle^{n_0}|-\rangle|+\rangle^{n_1}|-\rangle|+\rangle^{n_2}\cdots|-\rangle|+\rangle^{n_{q-1}}|-\rangle|+\rangle^{n_q}, \tag{13}$$

TABLE I. State evolution of the Turing head for $M=1$ and initial states $|\mathcal{P}_0^j\rangle$: $\lambda_y^m(\mathcal{P}_0^j)=Y_m^{(j)}$, $\lambda_z^m(\mathcal{P}_0^j)=Z_m^{(j)}$, $j=1$ (aperiodic), and $j=2$ (periodic).

$Y_0^{(1)}=\sin\varphi_0$	$Y_0^{(2)}=Y_0^{(1)}$
$Z_0^{(1)}=-\cos\varphi_0$	$Z_0^{(2)}=Z_0^{(1)}$
$Y_1^{(1)}=Y_2^{(1)}=\sin(\varphi_0+\alpha)$	$Y_1^{(2)}=-Y_2^{(2)}=Y_1^{(1)}$
$Z_1^{(1)}=Z_2^{(1)}=-\cos(\varphi_0+\alpha)$	$Z_1^{(2)}=Z_2^{(2)}=Z_1^{(1)}$
$Y_3^{(1)}=Y_4^{(1)}=\sin(\varphi_0+2\alpha)$	$Y_3^{(2)}=-Y_4^{(2)}=-Y_0^{(2)}$
$Z_3^{(1)}=Z_4^{(1)}=-\cos(\varphi_0+2\alpha)$, etc.	$Z_3^{(2)}=Z_4^{(2)}=Z_0^{(2)}$, etc.

with $n_i=0,1,2,\ldots$, contains $q|-\rangle$ states, where $\Sigma_{i=0}^{q}n_i+q=M, q=$ odd for M odd or even, while q can be even only for M even, satisfying

$$\sum_{i=0}^{q/2} n_{2i}=\frac{M-q}{2}. \tag{14}$$

Otherwise $|\varphi_m(S)\rangle|\mathcal{P}_0^j\rangle$ generates an aperiodic orbit (i.e., an effective rotation controlled by α). The aperiodic (''quasi-periodic'') primitives also become strictly periodic, if α is a rational multiple of π.

Any initial state with S in the pure state $|\varphi_0(S)\rangle$ can thus be written

$$|\psi_0\rangle=\sum_{j=1}^{2^M} a_j|\varphi_0(S)\rangle|\mathcal{P}_0^j\rangle, \tag{15}$$

i.e., $|\psi_0\rangle$ can be specified by the coefficients $\{a_j\}$. With Eq. (15), and using the orthogonality of the $|\mathcal{P}_0^j\rangle$, the resulting motion of the Turing head depends only on the modulus of a_j, and is given by [cf. Eqs. (5) and (10)]

$$\lambda_k^m(\psi_0)=\sum_{j=1}^{2^M} |a_j|^2\lambda_k^m(\mathcal{P}_0^j). \tag{16}$$

This decomposition can be seen as an intuitive example for quantum parallelism: The individual Turing head performs exponentially many primitive trajectories ''in parallel.'' We may restrict the sum in Eqs. (15) and (16) to the periodic (aperiodic) primitives only. Equal weight superpositions of

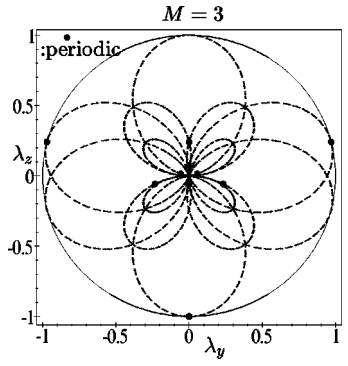

FIG. 2. Equal-weight superpositions ($a_j=\frac{1}{2}$) of four periodic (four aperiodic) orbits for $|\psi_0\rangle=|0000\rangle$, $M=3$, and total step number $m=3000$. The equal-weight superposition $(1/\sqrt{2})$ of these two, in turn, generates the pattern for initial state $|0000\rangle$ (see Fig. 3 for $M=3$); $\alpha=\pi/\sqrt{3}$.

TABLE II. Recursion relations for the reduced state evolution of S in the case of $|\psi_0\rangle=|00\cdots0\rangle$ and $\alpha_1=\alpha_2=\cdots=\alpha_M$. Let $Y_m=Y_{m,M}$, $Z_m=Z_{m,M}$, $Z_{m,0}:=-1$, and $m':=m-4p+2$, where p is the cycle number for step m; $m=n+2M(p-1)$, $n=1,2,\ldots,2M$. $Y_0=0$, $Y_1=\sin\alpha$, $Z_0=-1$, and $Z_1=-\cos\alpha$.

$Y_m=-Y_1Z_{m-1}-Z_1Y_{m-1}$	$n=$ odd
$Y_{m,M}=Y_{m-1,M}+Y_1Z_{m',M-2}$	$n=$ even $\neq 2M$
$Y_{m,M}=Y_{m-1,M}-Y_1(-Z_1)^{M-1}$	$n=2M$, $p=$ odd
$Y_{m,M}=Y_{m-1,M}$	$n=2M$, $p=$ even
$Z_m=-Z_1Z_{m-1}+Y_1Y_{m-1}$	$n=$ odd
$Z_m=-Z_1Z_{m-2}+Y_1Y_{m-2}$	$n=$ even

the four periodic (four aperiodic) orbits lead to the isolated point (quasi-one-dimensional) patterns as shown in Fig. 2 $(M=3,\varphi_0=0)$. The special equal-weight superposition with $a_j=(1/2^M)^{1/2}$ corresponds to the initial state $|\psi_0\rangle=|\varphi_0(S)\rangle\otimes|00\cdots0\rangle$, which is a complete product state. There are other nonproduct states, however, leading to the same equal-weight result for the Turing head, i.e., to the same pattern.

For $|\psi_0\rangle=|00\cdots0\rangle$, the typical initial state also for quantum computation [6], and for large M the construction of the Turing-head motion based on the decomposition approach (2^M primitives with equal weight) becomes impractical. Surprisingly, the Bloch vector of S can easily be found for any M and any step number $m=n+2M(p-1)$ from

$$\lambda_x^m=0,$$

$$\lambda_y^m=Y_{m,M}(\alpha),$$

$$\lambda_z^m=Z_{m,M}(\alpha) \tag{17}$$

using the recursion relations (Table II). Alternatively, the Bloch vector $\vec{\lambda}^m$ can be calculated directly from the initial state [14]. The resulting geometrical patterns for $M=1$, 2, 3,

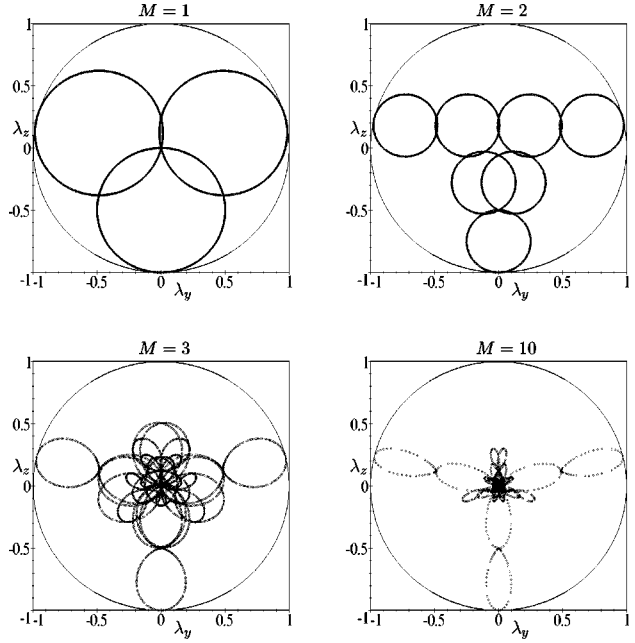

FIG. 3. Turing-head patterns for $|\psi_0\rangle|00\cdots0\rangle$, $M=1$, 2, 3, and 10, and the total step number $m=3000$; $\alpha=\pi/\sqrt{3}$.

and 10 are shown in Fig. 3, including all steps up to $m=3000$. These patterns, reminiscent of Poincaré sections in classical phase spaces (for open quantum systems compare [15]), decompose into various submanifolds (which reflect higher-order invariants). In the process of their buildup, the Bloch vector $\vec{\lambda}^m$ jumps between these submanifolds, just as between the discrete points of the corresponding superposition of all the periodic orbits (a one-to-one correspondence; compare Fig. 2); the latter thus play an important role reminiscent of Gutzwiller's *periodic-orbit theory* [16]. For $M=1$ and 2 the sub-manifolds are circles with radius r and center $\vec{c}_j$, defining the invariants I

$$I(\vec{\lambda})=\prod_{j=1}^{2^{M+1}}(|\vec{\lambda}-\vec{c}_j|-r)=0 \tag{18}$$

(for $\varphi_0=0$ two of the circles coincide). We note in passing that the initial state $|10\cdots0\rangle$ generates a Turing-head trajectory with $\vec{\lambda}^m$ of Fig. 3 replaced by $-\vec{\lambda}^m$ (the individual tape spin may be in any state $|0\rangle,|1\rangle$). The unitary evolution of a mixed state can thus be constructed as weighted combinations of these trajectories, at each step m. They lead to ''shrunk'' patterns.

The unitary transformations $\hat{U}_\alpha(S)$ and $\hat{U}(S,\mu)$ do not commute for $\alpha\neq0$: Even without introducing any time parameters, the sequence of transformation thus defines a specific order. This ordering can be made explicit by associating a time Δt with each step m. The Fourier transform of this discrete dynamics (underlying the buildup of the Turing-head pattern) will thus give complementary information, accessible to spectroscopy. This would amount to testing the ''nonclassicality'' of the respective trajectory rather than testing the nonclassicality of states. Absolute time scales become relevant as we compare Δt with the decoherence time τ_c. Even short times τ_c might be overcome by running the Turing machine fast enough, i.e., by choosing $2M\Delta t\ll\tau_c$. Note that the Turing-head dynamics is robust with respect to phase changes of the Turing-tape states.

In conclusion, we have shown that the QTM architecture allows for a discrete dynamical evolution which, when viewed from the reduced subspace of the Turing head, appears as some highly ordered geometric pattern. For specific initial states (''input''), these patterns (''output'') can be easily calculated for any tape size. They constitute a sensitive local test for the functioning of the total network in its exponentially large Hilbert space. The ''output'' becomes available for any large enough observation period, and does not suffer from the notorious ''halting problem'' [17]. These findings, we believe, are the first concrete results pertaining to QTM's, a field which up to now has not shown much potential for future applications.

We would like to thank C. Granzow, A. Otte, and R. Wawer for stimulating discussions.

[1] A. J. Lichtenberg and M. A. Lieberman, *Regular and Stochastic Motion* (Springer-Verlag, New York, 1983).
[2] R. C. Hilborn, *Chaos and Nonlinear Dynamics* (Oxford University Press, New York, 1994).
[3] S. Wolfram, Phys. Rev. Lett. **54**, 735 (1985).
[4] G. Mahler and V. A. Weberruss, *Quantum Networks: Dynamics of Open Nanostructures*, 2nd ed. (Springer-Verlag, Berlin, 1998).
[5] R. P. Feynman, Int. J. Theor. Phys. **21**, 467 (1982).
[6] D. P. DiVincenzo, Science **270**, 255 (1995).
[7] A. Ekert and R. Jozsa, Rev. Mod. Phys. **68**, 733 (1996).
[8] S. Lloyd, Science **273**, 1073 (1996).
[9] D. Deutsch, Proc. R. Soc. London, Ser. A **400**, 97 (1985).
[10] D. Deutsch, Proc. R. Soc. London, Ser. A **425**, 73 (1989).
[11] P. Benioff, Phys. Rev. Lett. **48**, 1581 (1982).
[12] P. Benioff, Phys. Rev. A **54**, 1106 (1996).
[13] P. Benioff, Fortschr. Phys. **46**, 423 (1998).
[14] G. Mahler and I. Kim, in *Lecture Notes in Computer Science* (Springer Verlag, New York, in press), Vol. 1509; also available as online e-print quant-ph/9803008.
[15] T. P. Spiller and J. F. Ralph, Phys. Lett. A **194**, 235 (1994).
[16] M. C. Gutzwiller, *Chaos in Classical and Quantum Mechanics* (Springer-Verlag, New York, 1990).
[17] J. M. Myers, Phys. Rev. Lett. **78**, 1823 (1997).